

Controlled Stoichiometric Incorporation of Ti(IV) into a Zr(IV) Pinacolate

Cecilia A. Zechmann, John C. Huffman, Kirsten Foltg, and Kenneth G. Caulton*[†]

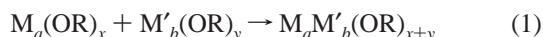
Department of Chemistry and Molecular Structure Center, Indiana University, Bloomington, Indiana 47405-4001

Received June 22, 1998

The first Ti/Zr mixed-metal alkoxide was synthesized by the reaction of equimolar amounts of $\text{Ti}(\text{O}^i\text{Pr})_4$ and $\text{Zr}_2(\text{OCMe}_2\text{CMe}_2\text{O})_2(\text{OCMe}_2\text{CMe}_2\text{OH})_4$ to give $\text{TiZr}_2(\text{OCMe}_2\text{CMe}_2\text{O})_4(\text{OCMe}_2\text{CMe}_2\text{OH})_2(\text{O}^i\text{Pr})_2$. The 1:1 (Ti:Zr) mixed-metal product was obtained by reaction of $\text{Ti}(\text{O}^i\text{Pr})_4$ and $\text{Zr}_2(\text{OCMe}_2\text{CMe}_2\text{O})_2(\text{OCMe}_2\text{CMe}_2\text{OH})_4$ (2:1 mole ratio, respectively) yielding $\text{Ti}_2\text{Zr}_2(\text{OCMe}_2\text{CMe}_2\text{O})_6(\text{O}^i\text{Pr})_4$. Both products were characterized by X-ray diffraction. Crystallographic data ($P2_1/c$ at $-164\text{ }^\circ\text{C}$) for $\text{TiZr}_2(\text{OCMe}_2\text{CMe}_2\text{O})_4(\text{OCMe}_2\text{CMe}_2\text{OH})_2(\text{O}^i\text{Pr})_2$: $a = 12.926(3)\text{ \AA}$, $b = 17.727(4)\text{ \AA}$, $c = 23.144(5)\text{ \AA}$, $\beta = 102.30(1)^\circ$ with $Z = 4$. Crystallographic data (PI at $-170\text{ }^\circ\text{C}$) for $\text{Ti}_2\text{Zr}_2(\text{OCMe}_2\text{CMe}_2\text{O})_6(\text{O}^i\text{Pr})_4 \cdot 2\text{CHCl}_3$: $a = 10.760(1)\text{ \AA}$, $b = 18.202(3)\text{ \AA}$, $c = 9.827(1)\text{ \AA}$, $\beta = 166.53(1)^\circ$ with $Z = 1$.

Introduction

Recent work in our group has involved the synthesis of heterometallic alkoxides which could be utilized as precursors to lead zirconium titanate, PZT.¹ This ferroelectric material has the general formula $\text{Ti}_{1-x}\text{Zr}_x\text{PbO}_3$ and exhibits a variety of physical and electrical properties which can be controlled, in part, by altering the group IV metal ratio, x .² The simplest synthetic strategy to such precursor compounds involves the combination of two or more different homometallic metal alkoxides (eq 1).^{3–5} However, the resulting aggregates some-



times dissociate upon dissolution or heating.^{4a,b} More complex synthetic routes often involve salt metathesis or acid–base reactions and, as such, may require the previous successful synthesis of suitable starting materials.^{6,7} For these reasons only a handful of metal alkoxides containing lead and titanium⁸ or lead and zirconium^{1,9} have been described, and as yet, no

alkoxides containing both titanium and zirconium or all three metals have been reported.

Less common is the method of reacting complexes containing different anionic oxygen-donor ligands (X) in addition to different metals (eq 2).^{10,11} As the aforementioned synthetic



methods have limitations in the range of feasible products, this underutilized “heteroleptic methodology” warrants a more thorough investigation. Such an approach may be more effective if the ligands have an appreciable disparity in acidity and/or steric bulk, rendering one of the metals more Lewis acidic. In our initial attempts we have employed a typical monodentate alkoxide (isopropoxide) and a vicinal diolate (pinacolate) which has displayed the ability to both chelate and bridge metal centers.¹² The diol, pinacol ($\text{HOCH}_2\text{CMe}_2\text{OH}$), is both more acidic ($\sim 2\text{ p}K_a$ units) and sterically less demanding than two isopropanol molecules due to the tethering of the methyl groups by the C_2 backbone. In addition to merely preparing a mixed-metal alkoxide, it was hoped that any general principles arising from this investigation may contribute to eventual synthetic control over precursor metal stoichiometries.

Experimental Section

General. All manipulations were carried out using standard Schlenk techniques or in an argon atmosphere glovebox. Tetrahydrofuran, benzene, and pentane were dried over sodium benzophenone ketyl.

[†] E-mail: caulton@indiana.edu.

- (1) (a) Teff, D. J.; Huffman, J. C.; Caulton, K. G. *Inorg. Chem.* **1995**, *34*, 2491. (b) Teff, D. J.; Huffman, J. C.; Caulton, K. G. *Inorg. Chem.* **1996**, *35*, 2981. (c) Teff, D. J.; Huffman, J. C.; Caulton, K. G. *J. Am. Chem. Soc.* **1996**, *118*, 4030.
- (2) Xu, Y. *Ferroelectric Materials and Their Applications*; North-Holland: New York, 1991.
- (3) (a) Meerwein, H.; Bersin, T. *Justus Liebigs Ann. Chem.* **1929**, 476, 113. (b) Kapoor, P. N.; Mehrotra, R. C. *Coord. Chem. Rev.* **1974**, *14*, 1. (c) Bradley, D. C.; Mehrotra, R. C.; Gaur, D. P. *Metal Alkoxides*; Academic Press: London, 1978.
- (4) (a) Mehrotra, R. C.; Agrawal, M. M. *J. Chem. Soc. A* **1967**, 1026. (b) Mehrotra, R. C.; Agrawal, M. M.; Kapoor, P. N. *J. Chem. Soc. A* **1968**, 2673. (c) Mehrotra, R. C.; Mehrotra, A. J. *J. Chem. Soc., Dalton Trans.* **1972**, 1203. (d) Bartley, W. G.; Wardlaw, W. J. *J. Chem. Soc.* **1958**, 422. (e) Samuels, J. A.; Lobkovsky, E. B.; Streib, W. E.; Foltg, K.; Huffman, J. C.; Zwanziger, J. W.; Caulton, K. G. *J. Am. Chem. Soc.* **1993**, *115*, 5093.
- (5) For a recent review, see: Veith, M.; Mathur, S.; Mathur, C. *Polyhedron* **1998**, *17*, 1005.
- (6) (a) Vaartstra, B. A.; Samuels, J. A.; Barash, E. H.; Martin, J. D.; Streib, W. E.; Gasser, C.; Caulton, K. G. *J. Organomet. Chem.* **1993**, *449*, 191. (b) Dubey, R. K.; Singh, A.; Mehrotra, R. C. *J. Organomet. Chem.* **1988**, *341*, 569. (c) Veith, M.; Mathur, S.; Huch, V. *J. Chem. Soc., Dalton Trans.* **1996**, 2485. (d) Veith, M.; Mathur, S.; Huch, V. *J. Am. Chem. Soc.* **1996**, *118*, 903. (e) Sogans, S.; Singh, A.; Bohra, R.; Mehrotra, R. C. *J. Chem. Soc., Chem. Commun.* **1991**, 738.

- (7) (a) Vaartstra, B. A.; Streib, W. E.; Caulton, K. G. *J. Am. Chem. Soc.* **1990**, *112*, 8593. (b) Vaartstra, B. A.; Huffman, J. C.; Streib, W. E.; Caulton, K. G. *Inorg. Chem.* **1991**, *30*, 3068.
- (8) (a) Chandler, C. D.; Hampden-Smith, M. J. *J. Chem. Mater.* **1992**, *4*, 1137. (b) Daniele, S.; Papiernik, R.; Hubert-Pfalzgraf, L. G. *Inorg. Chem.* **1995**, *34*, 628.
- (9) Vaartstra, B. A. *Mater. Res. Soc. Symp. Proc.* **1993**, 282, 689.
- (10) (a) Labrize, F.; Hubert-Pfalzgraf, L. G.; Daran, J. C.; Halut, S. *Polyhedron* **1996**, *15*, 2707. (b) Sirio, C.; Poncelet, O.; Hubert-Pfalzgraf, L. G.; Daran, J. C.; Vaissermann, J. *Polyhedron* **1992**, *11*, 177.
- (11) Kessler, V. G.; Hubert-Pfalzgraf, L. G.; Halut, S.; Daran, J.-C. *J. Chem. Soc., Chem. Commun.* **1994**, 705.
- (12) Zechmann, C. A.; Huffman, J. C.; Caulton, K. G. *Chem. Mater.*, submitted.

Chloroform was dried over P₂O₅. All solvents were distilled and stored over molecular sieves and under a nitrogen or argon atmosphere. Pinacol was purchased from Aldrich and sublimed prior to use. Zr₂(OⁱPr)₈(HOⁱPr)₂ was obtained from Aldrich and recrystallized from a 5% HOⁱPr/pentane solution. The alcohol-free analogue, [Zr(OⁱPr)₄]₃, was obtained by heating (100 °C) solid Zr₂(OⁱPr)₈(HOⁱPr)₂ under vacuum for several hours. Ti(OⁱPr)₄ was used as received from Aldrich. Zr₂(OCMe₂CMe₂O)₂(OCMe₂CMe₂OH)₄ was prepared as previously described.¹² ¹H NMR spectra were obtained on a Varian Inova 400 MHz spectrometer. All chemical shifts were referenced to residual solvent peaks.

Synthesis of TiZr₂(OCMe₂CMe₂O)₄(OCMe₂CMe₂OH)₂(OⁱPr)₂. A solution of 0.583 g of Ti(OⁱPr)₄ (2.05 mmol) in 15 mL of THF was transferred by cannula to a stirred solution of 1.80 g of Zr₂(OCMe₂CMe₂O)₂(OCMe₂CMe₂OH)₄ (2.04 mmol) in 30 mL of THF. The reaction was allowed to proceed at room temperature for 5–10 min after which the solvent was removed in vacuo, leaving a white solid. Yield: 2.07 g (97%). Elemental analysis for C₄₂H₈₈O₁₄TiZr₂: (calcd) 48.16, C; 8.47, H; (found) 48.30, C; 7.98, H. ¹H NMR (–15 °C, THF-*d*₈) (resonances arise from methyls of pinacolite ligands unless otherwise noted): 9.72 ppm (s, 1H, OC(CH₃)₂C(CH₃)₂OH), 5.08 (s, 1H, OC(CH₃)₂C(CH₃)₂OH), 4.93 (sept, 1H, TiOCH(CH₃)₂), 4.75 (sept, 1H, TiOCH(CH₃)₂), 1.73 (s, 3H), 1.67 (s, 3H), 1.60 (s, 3H), {1.52, 1.51, 1.50, 1.48, 1.47} (singlets total of 21H), 1.44 (s, 3H), {1.36, 1.34, 1.33, 1.32, 1.30, 1.28, 1.27, 1.25} 30H singlets and 3 × (d, 3H, TiOCH(CH₃)₂), 1.15 (d, 3H, TiOCH(CH₃)₂), 1.13 (s, 3H), 1.02 (s, 3H), 0.96 (s, 3H).

Synthesis of Ti₂Zr₂(OCMe₂CMe₂O)₆(OⁱPr)₄. Ti(OⁱPr)₄ (0.432 g, 1.52 mmol) was weighed into a vial in an argon atmosphere glovebox. Zr₂(OCMe₂CMe₂O)₂(OCMe₂CMe₂OH)₄ (0.671 g, 0.760 mmol) was weighed into a Schlenk flask, and 5 mL of THF was added to form a slurry. The Ti(OⁱPr)₄ was added dropwise to the slurry, which slowly cleared to give a colorless solution. A THF wash (2–3 mL) of the vial was added to the Schlenk flask to deliver any residual Ti(OⁱPr)₄. In less than 30 s, colorless crystals began forming. The solvent was removed in vacuo, leaving a white powder. Yield: 0.845 g (91%). Elemental anal. for C₄₈H₁₀₀O₁₆Ti₂Zr₂: (calcd) 47.59, C; 8.32, H; (found) 47.47, C; 7.99, H. ¹H NMR (–20 °C, THF-*d*₈) (resonances arise from methyls of pinacolite ligands unless otherwise noted): 4.94 ppm (sept, 2H, TiOCH(CH₃)₂), 4.73 (sept, 2H, TiOCH(CH₃)₂), 1.72 (s, 6H), 1.68 (s, 6H), 1.61 (s, 6H), 1.59 (s, 6H), 1.51 (s, 6H), 1.49 (s, 6H), 1.41 (s, 6H), 1.33 (d, 6H, TiOCH(CH₃)₂), {1.28, 1.27, 1.24, 1.23} (3 × (s, 6H) and 2 × (d, 6H)), 1.15 (d, 6H, TiOCH(CH₃)₂), 1.01 (s, 6H), 0.98 (s, 6H).

Reaction of Ti(OⁱPr)₄ with TiZr₂(OCMe₂CMe₂O)₄(OCMe₂CMe₂OH)₂(OⁱPr)₂. TiZr₂(OCMe₂CMe₂O)₄(OCMe₂CMe₂OH)₂(OⁱPr)₂ (0.116 g, 0.111 mmol) was added to a solution of 0.0315 g of Ti(OⁱPr)₄ (0.111 mmol) in ~1 mL of THF. The resulting mixture almost completely dissolved (~30 s), after which a white precipitate began to form. After 1 h, a small amount of the mixture was transferred to an NMR tube and more THF-*d*₈ was added (~0.5 mL), to give a clear colorless solution. ¹H NMR revealed the major product (>80%) to be Ti₂Zr₂(OCMe₂CMe₂O)₆(OⁱPr)₄.

Attempted Reaction of Ti(OⁱPr)₄ with Zr₂(OⁱPr)₈(HOⁱPr)₂. Zr₂(OⁱPr)₈(HOⁱPr)₂ (0.027 g) was added to a vial containing 0.020 g of Ti(OⁱPr)₄ (0.070 mmol). Toluene-*d*₈ (0.7 mL) was added to form a colorless solution, which was then stirred at room temperature. After 4 h, the solution was transferred to an NMR tube for analysis, which revealed only resonances of the unchanged components. ¹H NMR (20 °C, toluene-*d*₈): 4.56 ppm (b, ZrOCH(CH₃)₂), 4.49 (sept, TiOCH(CH₃)₂), 1.37 (d, ZrOCH(CH₃)₂), 1.24 (d, TiOCH(CH₃)₂). ¹H NMR (–20 °C, toluene-*d*₈): 5.08 ppm (b, ZrOCH(CH₃)₂), 4.54 (sept, TiOCH(CH₃)₂), 4.42 (b, ZrOCH(CH₃)₂), 1.33 (d, ZrOCH(CH₃)₂), 1.26 (d, TiOCH(CH₃)₂).

Attempted Reaction of Ti(OⁱPr)₄ with [Zr(OⁱPr)₄]₃. [Zr(OⁱPr)₄]₃ (0.023 g, 0.023 mmol) was added to a vial containing 0.020 g of Ti(OⁱPr)₄ (0.070 mmol). Toluene-*d*₈ (0.7 mL) was added to form a colorless solution, which was then stirred at room temperature. After 4 h, the solution was transferred to an NMR tube for analysis. Only the unreacted reagent signals were observed. ¹H NMR (20 °C, toluene-*d*₈): 4.60 ppm (sept, ZrOCH(CH₃)₂), 4.49 (sept, TiOCH(CH₃)₂), 1.42

Table 1. Crystallographic Data

formula compound	C ₄₂ H ₈₈ O ₁₄ TiZr ₂ 1	C ₄₈ H ₁₀₀ O ₁₆ Ti ₂ Zr ₂ ·2CHCl ₃ 2
<i>a</i> , Å	12.926(3)	10.760(1)
<i>b</i> , Å	17.727(4)	18.202(3)
<i>c</i> , Å	23.144(5)	9.827(1)
α, deg		93.08(1)
β, deg	102.30(1)	116.53(1)
γ, deg		100.79(1)
<i>V</i> , Å ³	5181.43	1670.84
<i>Z</i>	4	1
fw	1047.48	1923.09
space group	<i>P</i> 2 ₁ / <i>c</i>	<i>P</i> 1̄
<i>T</i> , °C	–164	–170
λ, Å	0.710 69	0.710 69
ρ _{calcd} , g/cm ³	1.343	1.441
μ(Mo Kα), cm ^{–1}	6.01	8.2
<i>R</i> (<i>F</i>) ^a	0.0553	0.0582
<i>R</i> _w (<i>F</i>) ^b	0.0521	0.0533

^a $R = \sum |F_o| - |F_c| / \sum |F_o|$, ^b $R_w = [\sum w(|F_o| - |F_c|)^2 / \sum w|F_o|^2]^{1/2}$ where $w = 1/\sigma^2(|F_o|)$.

(d, ZrOCH(CH₃)₂), 1.24 (d, TiOCH(CH₃)₂). ¹H NMR (–20 °C, toluene-*d*₈): 4.58 ppm (b, ZrOCH(CH₃)₂), 4.54 (sept, TiOCH(CH₃)₂), 1.42 (d, ZrOCH(CH₃)₂), 1.26 (d, TiOCH(CH₃)₂).

Reaction of Ti₂Zr₂(OCMe₂CMe₂O)₆(OⁱPr)₄, 2, with HOCMe₂CMe₂OH. Ti₂Zr₂(OCMe₂CMe₂O)₆(OⁱPr)₄ (0.431 g, 0.352 mmol) and 0.168 g of HOCMe₂CMe₂OH (1.42 mmol) were weighed into a Schlenk flask. THF (10 mL) was added to form a slightly cloudy solution, which was refluxed overnight and cooled to room temperature to give a clear, colorless solution. The solvent was removed in vacuo, leaving a white solid. The material was then washed with three 5 mL portions of pentane and dried under vacuum. Yield: 0.254 g, 65% (calculated for product identified). ¹H NMR indicated pure Zr₂(OCMe₂CMe₂O)₂(OCMe₂CMe₂OH)₄.

Solid State Structure of TiZr₂(OCMe₂CMe₂O)₄(OCMe₂CMe₂OH)₂(OⁱPr)₂. A suitable crystal was mounted in a nylon fiber loop at the end of a glass fiber and was quickly transferred to the goniostat, where it was cooled to –164 °C for characterization and data collection. Crystallographic data is summarized in Table 1. A preliminary search for peaks followed by analysis using DIRAX and TRACER revealed a primitive monoclinic unit cell. Subsequent solution and refinement confirmed the space group *P*2₁/*c*. The structure was solved using direct methods and Fourier techniques. The three metal atoms were obtained from the initial *E*-map. The remaining non-hydrogen atoms were located in iterations of least-squares refinement followed by difference Fourier calculations. Almost all of the hydrogen atoms were located, at least one on each of the methyl groups as well as the two hydrogen atoms involved in the hydrogen bonding. All of the hydrogen atoms on carbon atoms were introduced in fixed idealized positions and were assigned isotropic thermal parameters equal to 1.0 plus the isotropic equivalent of the parent atom. The final full-matrix least-squares refinement was carried out using anisotropic thermal parameters on all non-hydrogen atoms and isotropic thermal parameters on the two hydrogen atoms which were refined, H(1) and H(62). The final difference Fourier was essentially featureless, the largest peak was 0.86 e/Å³, 0.9 Å from Zr(2), and the deepest hole was –0.51 e/Å³.

Solid State Structure of Ti₂Zr₂(OCMe₂CMe₂O)₆(OⁱPr)₄·2CHCl₃. A square fragment was cleaved from a flat, diamond-shaped crystal and affixed to the end of a glass fiber using silicone grease. It was then transferred to the goniostat where it was cooled to –170 °C for characterization and data collection. Crystallographic data is summarized in Table 1. A systematic search of a limited hemisphere of reciprocal space located a set of diffraction maxima with no symmetry or systematic absences indicating a triclinic space group. Subsequent solution and refinement confirmed the centrosymmetric space group *P*1̄. The structure was readily solved by direct methods (MULTAN78) and Fourier techniques. Hydrogen atoms were clearly visible in a difference Fourier phased on the non-hydrogen atoms and were included as isotropic contributors for the final cycles of refinement. The molecule lies at a center of inversion, and a CHCl₃ solvent molecule is

present in the asymmetric unit. A final difference Fourier was featureless, the largest peaks ($1.3 \text{ e}/\text{\AA}^3$) being in the vicinity of the CHCl_3 solvent.

Results

Synthesis and Characterization of $\text{TiZr}_2(\text{OCMe}_2\text{OCMe}_2\text{O})_4(\text{OCMe}_2\text{CMe}_2\text{OH})_2(\text{O}^i\text{Pr})_2$. Addition of a THF solution containing $\text{Ti}(\text{O}^i\text{Pr})_4$ to a stirred THF solution of an equimolar amount of $\text{Zr}_2(\text{OCMe}_2\text{CMe}_2\text{O})_2(\text{OCMe}_2\text{CMe}_2\text{OH})_4$ gave the 1:2 (Ti:Zr) product. X-ray crystallography identified the material as $\text{TiZr}_2(\text{OCMe}_2\text{OCMe}_2\text{O})_4(\text{OCMe}_2\text{CMe}_2\text{OH})_2(\text{O}^i\text{Pr})_2$. Thus, two isopropoxides deprotonate two singly protonated pinacolates to liberate isopropanol. The room temperature ^1H NMR revealed several broad resonances in the methyl region, two distinct but slightly broad methine peaks, and two peaks further downfield arising from the hydroxyl protons. Upon cooling to -15°C the spectrum sharpened significantly, but the large number of overlapping methyl signals precluded complete resolution of the expected 28 methyl groups (a total of 21 peaks were observed with only 8 of these having the intensity of a single methyl). Integration of the overlapping regions against the available resolved singlets was consistent with a total of 28 methyl groups. Because this is the number of methyl groups expected for the static structure observed in the solid state, the molecule is likely intact in solution, displaying no fluxional behavior which could result in higher symmetry. The location of the remaining three unresolved ^iPr methyl doublets was accomplished through sequential selective decoupling of the methine protons. At all temperatures the hydroxyl proton resonances possessed significantly different chemical shifts (5.08 and 9.72 ppm at -15°C). As chemical shift can have a large dependence on acid strength, it is reasonable to suggest that the downfield resonance is due to H1 (it is on an oxygen (O7) which is covalently bound to a metal center (Zr1) and therefore significantly more acidic), while the upfield resonance arises from the hydroxyl proton on the pendant ligand (H62 on O47).

It should also be noted that this material is a kinetic product and will slowly disappear if left in solution at room temperature for extended periods of time.¹³ Unfortunately, the product resulting from this transformation (made in quantitative yield by reflux in THF overnight) is significantly more soluble, and all attempts at crystallization were unsuccessful.

Synthesis and Characterization of $\text{Ti}_2\text{Zr}_2(\text{OCMe}_2\text{CMe}_2\text{O})_6(\text{O}^i\text{Pr})_4$. Addition of 2 equiv of $\text{Ti}(\text{O}^i\text{Pr})_4$ to a slurry of $\text{Zr}_2(\text{OCMe}_2\text{CMe}_2\text{O})_2(\text{OCMe}_2\text{CMe}_2\text{OH})_4$ in a minimal amount of THF or CHCl_3 gave an initially colorless solution from which crystals grew in just minutes. The 1:1 (Ti:Zr) product, **2**, could also be obtained by reaction of **1** with an equimolar amount of $\text{Ti}(\text{O}^i\text{Pr})_4$. High-quality crystals of **2** could be obtained by slow cooling of a saturated solution (THF or CHCl_3). X-ray crystallography identified the material as $\text{Ti}_2\text{Zr}_2(\text{OCMe}_2\text{CMe}_2\text{O})_6(\text{O}^i\text{Pr})_4$, which is the product of replacement of all four hydroxyl protons. Elemental analysis was consistent with this formulation. The room temperature ^1H NMR revealed only a very broad asymmetric peak in the methyl region as well as a single peak corresponding to the methine protons. Upon cooling to -20°C the methyl region resolved into 9 singlets corresponding to the methyl groups of the pinacolate ligands and 2 doublets corresponding to the methyl groups of the isopropoxides. The remaining 3 singlets and 2 doublets were

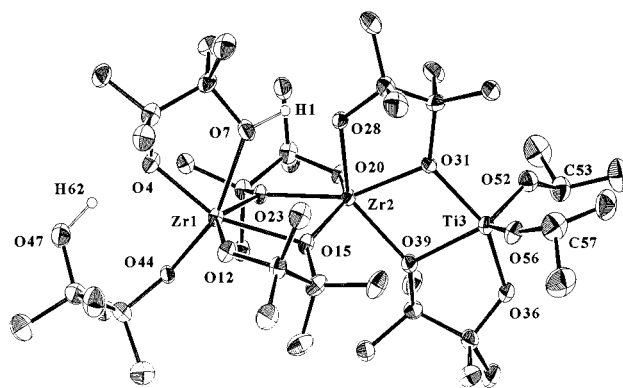


Figure 1. ORTEP representation of $\text{TiZr}_2(\text{OCMe}_2\text{OCMe}_2\text{O})_4(\text{OCMe}_2\text{CMe}_2\text{OH})_2(\text{O}^i\text{Pr})_2$ showing 50% probability thermal ellipsoids. Methyl protons are omitted for clarity.

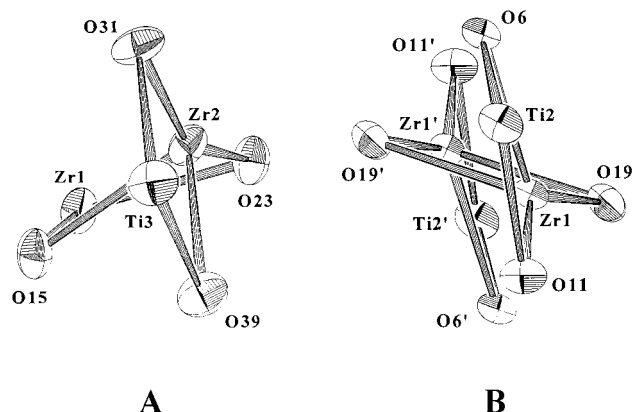


Figure 2. (A) ORTEP representation of the metal–oxygen core of $\text{TiZr}_2(\text{OCMe}_2\text{OCMe}_2\text{O})_4(\text{OCMe}_2\text{CMe}_2\text{OH})_2(\text{O}^i\text{Pr})_2$ and (B) ORTEP representation of the metal–oxygen core of $\text{Ti}_2\text{Zr}_2(\text{OCMe}_2\text{CMe}_2\text{O})_6(\text{O}^i\text{Pr})_4$ showing 50% probability thermal ellipsoids.

overlapping in the 1.28–1.23 ppm region and could not be resolved. Since the 24 pinacolate methyl groups give rise to just 12 resonances, the low-temperature solution structure must contain a 2-fold symmetry element in keeping with the observed solid state structure. At higher temperatures ($>20^\circ\text{C}$) the spectrum broadens and the methine signals coalesce, suggesting the occurrence of a fluxional process which, at the very least, equilibrates the isopropoxides.

Solid State Structure of $\text{TiZr}_2(\text{OCMe}_2\text{CMe}_2\text{O})_4(\text{OCMe}_2\text{CMe}_2\text{OH})_2(\text{O}^i\text{Pr})_2$, **1.** $\text{TiZr}_2(\text{OCMe}_2\text{CMe}_2\text{O})_4(\text{OCMe}_2\text{CMe}_2\text{OH})_2(\text{O}^i\text{Pr})_2$ crystallizes out of THF in the space group $P2_1/c$. An ORTEP representation of the compound is shown in Figure 1 with selected bond distances and angles listed in Table 2. Each zirconium remains six coordinate (as in $\text{Zr}_2(\text{OCMe}_2\text{CMe}_2\text{O})_2(\text{OCMe}_2\text{CMe}_2\text{OH})_4$) while the titanium has coordination number 5. While all six ligand oxygens surrounding Zr1 and Zr2 come solely from the pinacolates, the titanium retains two terminal isopropoxide ligands. The $\text{Zr1}-\text{Zr2}-\text{Ti3}$ angle is 151.6° , and each pair of metals is bridged by two pinacolate oxygens, all arising from different ligands. Shown in Figure 2A is an ORTEP representation of the three metal atoms and their four bridging oxygens. The two four-atom planes, each formed by a pair of metals and the two oxygens that bridge them, have a dihedral angle of 79.5° .

The six pinacolates are found in a total of five bonding environments. One ligand is bound by a single oxygen to zirconium (η^1) while its pendant hydroxyl group is involved in hydrogen bonding, a second is chelating zirconium (η^2), and the remaining four are chelating one metal and bridging to a

(13) ^1H NMR in $\text{THF}-d_8$ revealed the growth of new peaks in the methine region in concert with the decrease in intensity of the previous resonances. The conversion becomes significant after 10–12 h at room temperature.

Table 2. Selected Distances (Å) and Angles (deg) for $\text{Ti}_2\text{Zr}_2(\text{OCMe}_2\text{CMe}_2\text{O})_4(\text{OCMe}_2\text{CMe}_2\text{OH})_2(\text{O}^i\text{Pr})_2$, **1**

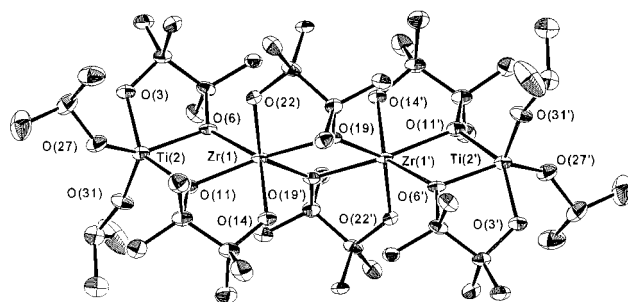
Distances (Å)			
Zr(1)···Zr(2)	3.5399(10)	Zr(2)–O(31)	2.135(3)
Zr(2)···Ti(3)	3.4117(12)	Zr(2)–O(39)	2.178(4)
Zr(1)–O(4)	2.028(4)	Ti(3)–O(31)	2.009(4)
Zr(1)–O(7)	2.293(4)	Ti(3)–O(36)	1.839(4)
Zr(1)–O(12)	1.980(4)	Ti(3)–O(39)	2.089(4)
Zr(1)–O(15)	2.280(3)	Ti(3)–O(52)	1.791(4)
Zr(1)–O(23)	2.133(3)	Ti(3)–O(56)	1.783(4)
Zr(1)–O(44)	1.936(4)	O(7)–H(1)	0.95(6)
Zr(2)–O(15)	2.137(4)	O(47)–H(62)	0.75(5)
Zr(2)–O(20)	1.965(3)	O(4)···O(47)	2.806(6)
Zr(2)–O(23)	2.182(3)	O(7)···O(28)	2.598(6)
Zr(2)–O(28)	2.039(3)		

Angles (deg)			
Zr(1)–Zr(2)–Ti(3)	151.584	O(20)–Zr(2)–O(39)	94.53(14)
O(4)–Zr(1)–O(7)	70.02(15)	O(23)–Zr(2)–O(28)	87.74(14)
O(4)–Zr(1)–O(12)	103.00(15)	O(23)–Zr(2)–O(31)	157.58(14)
O(4)–Zr(1)–O(15)	154.20(14)	O(23)–Zr(2)–O(39)	131.30(13)
O(4)–Zr(1)–O(23)	110.36(14)	O(28)–Zr(2)–O(31)	72.86(14)
O(4)–Zr(1)–O(44)	90.63(15)	O(28)–Zr(2)–O(39)	140.76(14)
O(7)–Zr(1)–O(12)	89.29(15)	O(31)–Zr(2)–O(39)	69.44(13)
O(7)–Zr(1)–O(15)	84.32(14)	O(31)–Ti(3)–O(36)	150.50(16)
O(7)–Zr(1)–O(23)	84.86(14)	O(31)–Ti(3)–O(39)	73.65(14)
O(7)–Zr(1)–O(44)	160.09(15)	O(31)–Ti(3)–O(52)	97.05(17)
O(12)–Zr(1)–O(15)	73.14(14)	O(31)–Ti(3)–O(56)	97.33(17)
O(12)–Zr(1)–O(23)	141.63(14)	O(36)–Ti(3)–O(39)	78.72(16)
O(12)–Zr(1)–O(44)	99.97(15)	O(36)–Ti(3)–O(52)	93.32(18)
O(15)–Zr(1)–O(23)	68.56(13)	O(36)–Ti(3)–O(56)	104.30(19)
O(15)–Zr(1)–O(44)	115.17(14)	O(39)–Ti(3)–O(52)	131.08(17)
O(23)–Zr(1)–O(44)	98.11(14)	O(39)–Ti(3)–O(56)	116.98(17)
O(15)–Zr(2)–O(20)	140.00(14)	O(52)–Ti(3)–O(56)	111.78(19)
O(15)–Zr(2)–O(23)	70.34(13)	Zr(1)–O(15)–Zr(2)	106.49(14)
O(15)–Zr(2)–O(28)	92.79(14)	Zr(1)–O(23)–Zr(2)	110.24(15)
O(15)–Zr(2)–O(31)	120.59(14)	Zr(2)–O(31)–Ti(3)	110.77(16)
O(15)–Zr(2)–O(39)	97.03(14)	Zr(2)–O(39)–Ti(3)	106.13(16)
O(20)–Zr(2)–O(23)	73.29(13)	Zr(1)–O(44)–C(45)	160.6(3)
O(20)–Zr(2)–O(28)	101.94(15)	Ti(3)–O(52)–C(53)	136.4(4)
O(20)–Zr(2)–O(31)	99.33(14)	Ti(3)–O(56)–C(57)	155.2(4)

second metal ($\eta^2-\mu_2$). Of the latter, two are chelating/bridging zirconium, one is chelating zirconium while bridging to titanium, and the last is chelating titanium and bridging to zirconium. Within a chelate, the O–M–O angles are quite small ($<80^\circ$). The O(36)–Ti(3)–O(39) angle is just slightly larger than the average O–Zr–O angle (78.7° vs 72.0°) corresponding to a shorter M–O bond distance. The average Zr–O distance is 2.11 Å, the longer involving the bridging (O15 and O23) and alcohol (O7) oxygens, as expected. The average Ti–O distance is slightly shorter at 1.90 Å with the shortest involving the isopropoxide oxygens (O52 and O56). This corresponds well with the relatively large Ti–O–C angles observed for the isopropoxides (136° and 155°) indicating possible π -donation from the oxygen lone pair.

There are two hydroxyl protons in the compound. One of these can be easily assigned to the pendant oxygen (O47) while the second proton was deduced to be on O7 due to a significantly longer Zr–O distance (2.293 Å). Additional evidence for this assignment comes from the short distance between O7 and O28 (2.598(6) Å) suggesting the presence of a hydrogen bond. A second hydrogen bond must exist between the pendant hydroxyl oxygen (O47) and O4, as they are separated by only 2.806 Å.

Solid State Structure of $\text{Ti}_2\text{Zr}_2(\text{OCMe}_2\text{CMe}_2\text{O})_6(\text{O}^i\text{Pr})_4$, **2.** $\text{Ti}_2\text{Zr}_2(\text{OCMe}_2\text{CMe}_2\text{O})_6(\text{O}^i\text{Pr})_4 \cdot 2\text{CHCl}_3$ crystallized in the centrosymmetric space group $P\bar{1}$. As there is a crystallographically imposed inversion center (between Zr1 and Zr1' in Figure 3), the asymmetric unit consists of half of the tetranuclear metal complex and one molecule of CHCl_3 . An ORTEP representation of the metal complex is displayed in Figure 3 with

**Figure 3.** ORTEP representation of $\text{Ti}_2\text{Zr}_2(\text{OCMe}_2\text{CMe}_2\text{O})_6(\text{O}^i\text{Pr})_4$ showing 50% probability thermal ellipsoids. Methyl protons are omitted for clarity.**Table 3.** Selected Distances (Å) and Angles (deg) for $\text{Ti}_2\text{Zr}_2(\text{OCMe}_2\text{CMe}_2\text{O})_6(\text{O}^i\text{Pr})_4$, **2**

Distances (Å)			
Ti(2)···Zr(1)	3.413	Zr(1)–O(6)	2.174(5)
Zr(1)···Zr(1')	3.549	Zr(1)–O(11)	2.164(5)
Ti(2)–O(3)	1.868(5)	Zr(1)–O(14)	1.984(5)
Ti(2)–O(6)	2.062(5)	Zr(1)–O(19)	2.234(5)
Ti(2)–O(11)	1.983(5)	Zr(1)–O(19')	2.113(5)
Ti(2)–O(27)	1.800(5)	Zr(1)–O(22)	1.976(5)
Ti(2)–O(31)	1.774(5)		

Angles (deg)			
Ti(2)–Zr(1)–Zr(1')	153.896	O(6)–Ti(2)–O(11)	73.37(19)
O(6)–Zr(1)–O(11)	67.77(18)	O(6)–Ti(2)–O(27)	141.69(23)
O(6)–Zr(1)–O(14)	136.67(20)	O(6)–Ti(2)–O(31)	107.85(23)
O(6)–Zr(1)–O(19)	94.76(19)	O(11)–Ti(2)–O(27)	95.36(23)
O(6)–Zr(1)–O(19')	137.37(18)	O(11)–Ti(2)–O(31)	103.66(24)
O(6)–Zr(1)–O(22)	92.08(19)	O(27)–Ti(2)–O(31)	110.40(26)
O(11)–Zr(1)–O(14)	72.91(20)	Ti(2)–O(3)–C(4)	121.6(5)
O(11)–Zr(1)–O(19)	151.01(18)	Zr(1)–O(6)–Ti(2)	107.34(21)
O(11)–Zr(1)–O(19')	130.14(18)	Zr(1)–O(6)–C(5)	136.6(4)
O(11)–Zr(1)–O(22)	96.67(20)	Ti(2)–O(6)–C(5)	113.4(4)
O(14)–Zr(1)–O(19)	85.68(19)	Zr(1)–O(11)–Ti(2)	110.71(22)
O(14)–Zr(1)–O(19')	96.90(20)	Zr(1)–O(11)–C(12)	116.2(4)
O(14)–Zr(1)–O(22)	110.14(20)	Ti(2)–O(11)–C(12)	131.8(5)
O(19)–Zr(1)–O(19')	70.60(20)	Zr(1)–O(14)–C(13)	126.0(5)
O(19)–Zr(1)–O(22)	72.20(19)	Zr(1)–O(19)–Zr(1')	109.40(20)
O(19')–Zr(1)–O(22)	131.53(20)	Zr(1)–O(19)–C(20)	114.3(4)
O(3)–Ti(2)–O(6)	78.53(21)	Zr(1)–O(19')–C(20')	135.2(4)
O(3)–Ti(2)–O(11)	143.15(23)	Zr(1)–O(22)–C(21)	127.5(4)
O(3)–Ti(2)–O(27)	92.09(23)	Ti(2)–O(27)–C(28)	138.5(5)
O(3)–Ti(2)–O(31)	107.36(24)	Ti(2)–O(31)–C(32)	163.8(6)

corresponding bond distances and angles summarized in Table 3. The metals of the complex zigzag with a 154° angle (Ti2–Zr1–Zr1') and are linked by three groups of two bridging pinacolate oxygen atoms. The bridging oxygens and the two metals they link form three separate planes. The two outer quadrilaterals (Ti(2), Zr(1), O(6), and O(11)) form planes that are parallel. The inner four-membered ring (formed by Zr(1), Zr(1'), O(19), and O(19')) defines a plane that intersects the first two planes at a 63.5° angle as can be seen in Figure 2B. The corresponding dihedral angle in **1** (Figure 2A) was slightly larger at 79.5° . This slight increase allows for closer O···O contacts in the hydrogen bond between O7 and O28 in **1**. The analogous distance in **2** (O14···O22') is much longer at 4.57 Å. Since there are no hydroxyl protons in **2**, this geometry/distance must be governed purely by steric factors.

Each of the pinacolate ligands is chelating a single metal and bridging by a single oxygen to a second metal ($\eta^2-\mu_2$). Two are chelating to zirconium and bridging to a second zirconium center while two more are chelating zirconium but bridging to titanium centers. The remaining two pinacolates are chelating titanium and bridging to zirconium. As in **1**, the isopropoxide ligands are bound only to titanium (two to each) and are

reverse reaction with free isopropanol will not be favored. Heteroleptic/heterometallic complexes have also been synthesized by the reaction of metal β -diketonates with metal alkoxides.¹⁰ In these complexes, the β -diketonates likewise bind in a chelating fashion, but the bridging oxygens are provided by the monodentate alkoxides. An argument can be made that the bridging position, aside from preferring the less-hindered ligand, also demands the more Lewis basic oxygen. In this regard, vicinal diolates are superior to β -diketonates, and their size can be tailored to successfully compete with a given monodentate alkoxide.

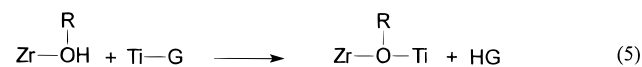
Shown in Scheme 1 are representations of the solid state structures of the starting compound, $Zr_2(OCMe_2CMe_2O)_2(OCMe_2CMe_2OH)_4$, **a**, and those of the two mixed-metal products. Their common and unique structural features are highlighted in these illustrations with the major difference involving the originally pendant ligands. While the local coordination environment around each of the zirconium atoms does not change ($Zr_2(OCMe_2CMe_2O)_6^{4-}$), the orientation of the original η^1 -pinacolates (with respect to zirconium) varies. This is readily seen by allowing the zirconium centers and the oxygens bridging them define a plane which separates each of the complexes into two hemispheres. In **1**, the two original η^1 ligands are in the same hemisphere (i.e., syn), while in **2**, they are in opposite hemispheres (i.e., anti). The fluxional process depicted (equilibrating **1** and **b**) is one possible mechanism by which this change in orientation (syn to anti) may be achieved. As there was evidence for some fluxional process occurring in the room temperature ¹H NMR of **2**, it is also possible that the orientation may oscillate following the second addition of $Ti(O^iPr)_4$.

The addition of the second titanium center to **1** gave the first complex in our pinacolate studies which contains no remaining acidic hydrogens. As such, **2** was reacted with 4 equiv of pinacol in an effort to replace the less Lewis basic isopropoxide.

Replacement of a terminal OⁱPr by a pendant O~OH could possibly allow for incorporation of a third metal in a manner analogous to that which gave **1** and **2**. Unfortunately, addition of excess pinacol resulted in the cleavage of **2** to give back $Zr_2(OCMe_2CMe_2O)_2(OCMe_2CMe_2OH)_4$ and an uncharacterized titanium species.

Conclusions

Synthesis of the first Ti/Zr mixed-metal alkoxides was achieved with a slight modification of an existing methodology. The synthetic method employed here, "replacement" of acidic alcohol protons on one metal by a second metal bearing a *different* acid-sensitive substituent (eq 5), succeeds under mild conditions (25 °C) to give a single product. Additionally,



exceptional synthetic stoichiometric control was possible as witnessed by the systematic addition of $Ti(O^iPr)_2^{2+}$ units to zirconium pinacolate. Several important factors contributed to the success of these reactions, including the presence of hydroxyl protons on one reagent (which imparted reactivity) and the chelating and bridging ability of the diolate ligand (which stabilized the product aggregate).

Acknowledgment. This work was supported by the U.S. Department of Energy.

Supporting Information Available: Tables listing detailed crystallographic data, atomic positional parameters, U_{ij} 's, and bond distances and angles (13 pages). Ordering information is given on any current masthead page.

IC980714Z